

Membrane admittance of cloned muscle cells in culture: use of a micropipet technique

Koji Asami¹, Shiro Takashima^{*}

Department of Bioengineering, University of Pennsylvania, 220 South 33rd Street, Suite 120 Hayden Hall, Philadelphia, PA 19104-6392, USA

(Received 26 April 1993)

(Revised manuscript received 31 August 1993)

Abstract

The impedance characteristics of muscle cells have been investigated by many investigators because of its unique features. The studies of the electrical properties of cloned cultured muscle cells, however, are scant and only a handful of papers have been published. In this report, the admittance of cultured Myoblast L6 cells was investigated. The capacitance and conductance of mononucleate myoblast cell membrane were found to be 2.2–2.5 $\mu\text{F}/\text{cm}^2$ and 50–60 $\mu\text{S}/\text{cm}^2$ and independent of frequency. The capacitance of 2.2 $\mu\text{F}/\text{cm}^2$ is larger than the widely accepted capacitance value for most of the biological cell membranes, i.e., 1 $\mu\text{F}/\text{cm}^2$. In contrast, those found for fused multinucleate myotubes are 5–6 $\mu\text{F}/\text{cm}^2$ and 0.4 mS/cm^2 and exhibited a marked frequency dependence. We postulate that the large and frequency dependent capacitance of myotubes does not arise from the surface membrane alone but is due to a tubule-like structure which may be similar to those found in frog muscles. Analysis of the results using an equivalent circuit demonstrates that the capacitance of myotubes is independent of frequency when the correction is made for the series resistances which are distributed in the lumen of tubule-like structure. An alternative explanation for the frequency dependent capacitance is based on the use of the transmission line theory or cable equation. The cable theory predicts that measured capacitance and conductance are inherently a function of frequency regardless of the nature of membrane capacitance and conductance if the dimension of cells is larger than or comparable to the propagation constant.

Key words: Membrane admittance; Electrical capacitance; Myoblast; Myotube; Cultured muscle cell

1. Introduction

The admittance characteristics of skeletal muscle fibers were investigated, in early research, using extracellular electrodes [1,2]. However, use of the intracellular glass microelectrodes led to a more physiologically important finding, i.e., the existence of a large admittance component due to transverse tubular membranes in addition to those due to the surface membrane. The initial work by Falk et al. [3] was followed by numerous investigations by Freygang et al. [4], Eisenberg et al. [5], Validiosa et al. [6], Vaughan et al. [7], Gage et al. [8] to name but a few. The unequivocal proof that the low frequency admittance component of muscle cells is indeed due to transverse tubules was

provided by the work by Eisenberg et al. [9,10] using electron-microscopy combined with impedance measurements. These investigators observed that the low frequency component of the admittance was eliminated nearly completely by the disruption of microtubules by glycerin treatment. Their additional finding was that the capacitance of the surface membrane was about 2–2.2 $\mu\text{F}/\text{cm}^2$, a value which is twice as large as the usual 1 $\mu\text{F}/\text{cm}^2$.

The advantage of the admittance or impedance technique is its unique ability to demonstrate the presence of the transverse tubular membrane more clearly than time domain techniques such as the analysis of action potential [11], or voltage-clamp ionic current measurements [12].

In recent years, the techniques of cell culture has been markedly advanced and cloned excitable cells such as neuroblastomas and myoblasts are now easily obtained in vitro in any laboratory which is equipped

^{*} Corresponding author. Fax: +1 (215) 5732071.

¹ Present address: Institute for Chemical Research, Kyoto University, Uji, Kyoto 611, Japan.

with simple cell culture facilities [13]. The advantage of the use of cultured myoblasts is the clearly separated two stages of growth of myoblasts, i.e., mononucleated myoblast cells and multinucleated myotubes. As discussed later, mononucleated myoblasts have a simple admittance characteristics and multinucleated myotubes exhibit a complex admittance behavior which remarkably resembles natural skeletal muscle cells. In this paper, we will discuss the electrical properties of admittance components, i.e., capacitance and conductance of the cultured myoblast cells using the micropipet technique, which was already discussed in a previous paper [14]. So far, the impedance characteristics of muscle fibers have been investigated almost exclusively using two glass microelectrodes as a current source and for voltage recording. The micropipet technique enables the impedance or admittance to be measured using only one electrode thus rendering the procedure somewhat simpler than the glass microelectrode method.

Mammalian skeletal muscles which were obtained from embryonic precursor cells (myoblast) grow exponentially in culture [15]. Myoblasts which are mononucleate cells start fusing and form multinucleate myotubes after the cessation of growth. Various skeletal muscle cell lines are now available and a cell line L6 which originates from rat thigh muscle was used in this study. Membrane electrical activities of the L6 cell were investigated extensively by Kidokoro [16–18] including resting membrane potential, action potential and membrane admittance. The resting membrane potential of L6 cells is about -70 mV and this value does not change significantly with the formation of myotubes. Action potentials can be elicited, only from myotubes, by the rising phase of hyperpolarizing pulses (anode break), a feature which is quite different from normal non-cultured excitable cells. The current–voltage diagram changes significantly when myoblasts form myotubes. In both cases, however, the sodium inward current having a negative slope was not observed. Although myotube cells are rarely able to contract spontaneously, they do not respond to external electrical stimuli. These are the major differences between natural full grown muscles and cultured myotubes.

Kidokoro [17] observed a capacitance and resistance of $1 \mu\text{F}/\text{cm}^2$ and 8 kohm cm^2 with myoblasts. The value of capacitance is, therefore, very similar to those reported for many other biological membranes whereas the membrane conductance of myoblasts is considerably smaller than those observed with other cells ($1\text{--}2 \text{ kohm cm}^2$). On the other hand Kidokoro found a much larger capacitance of $5 \mu\text{F}/\text{cm}^2$ and a resistance of 12 kohm cm^2 for myotubes. The large capacitance of myotubes is similar to the capacitance of transverse tubules of frog skeletal muscles (see Refs. [3–9]). Kidokoro suggests the existence of a tubule-like structure

in L6 myotubes in view of the large capacitance he observed.

During the exponential growth, myoblast cells remain mononucleated single cells. Only when myoblast cells cease to grow, cells begin to fuse and form multinucleated myotubes. Therefore, the advantage of using cultured myoblast cells is the ability to separate distinctly different two stages of growths and study the electrical and physiological properties independently. The separation of the admittances of surface and tubular membranes is difficult and subject to uncertainty when excised grown muscle fibers are used [7,8]. In addition, excised muscle single fibers includes myotendon junctions. Milton et al. [19] reported that the end of muscle fiber produces a large capacitance which may under certain conditions render the interpretation of capacitance measurement data more difficult. Cultured multinucleated myotubes, on the other hand, have a uniform structure and we are able to measure the admittance of fused cells without the complication caused by the myotendon junction thus rendering the interpretation more straight forward.

The aim of our work is the accurate determination of the capacitance and conductance of myoblast membrane in order to establish their frequency spectra between 1 Hz and 1 KHz . Kidokoro measured only the total capacitance using the square pulse technique and the problem of frequency dependence of the capacitance and conductance was not addressed in his reports. The determination of capacitance and conductance in a wide frequency range often provide us with much more information than total capacitance measurements in time domain.

2. Materials and methods

2.1. Cell culture

The cell line L6 was purchased from ATCC (Rockville, MD). Myoblast cells were cultured in Dulbecco's modified Eagle's Medium (DMEM) with 10% foetal calf serum at 37°C in an atmosphere of 5% CO_2 (Kidokoro used 12% CO_2).

2.2. Electrode

Glass micropipets were fabricated in the same way as for patch clamp pipets [20]. The tip impedance of these pipets is normally $10\text{--}15 \text{ Mohms}$. A micropipet filled with phosphate buffer solution with pH 7.2 were pressed against the cell membrane with gentle suction. After a tight seal was established, admittance measurements were made with the cell-attached configuration. The mean values of capacitances and conductances thus obtained were used for correction of electrode tip

capacitance and leakage conductance. After these measurements, a stronger suction was applied to establish a whole cell configuration. Admittance measurements were repeated with the whole cell configuration using the same cell. A silver-silver chloride wire was used as an external electrode.

2.3. Electrical apparatus

The electrical apparatus used in this experiment was described in detail in a previous paper [13] and was used without further modifications. As described, the output voltage V_o and input voltage V_i were sampled using an A/D converter (Lab Master, 30 kHz 12 bits resolution, Scientific Solutions, Solon, OH). The total data acquisition time was less than 60 s when 31 frequency points were scanned between 1 Hz and 1 kHz. Collected data points were fitted to sinusoidal wave forms by the least square minimization method to determine the amplitude (A) and phase angle (θ) of output voltage (V_o) relative to the input voltage (V_i). The system used is depicted schematically in Fig. 1. Based on the circuit illustrated in this figure, we can relate the voltage ratio V_o/V_i and phase angle θ to the sample admittance (Y_s) and feedback admittance (Y_f) as shown by the following equation.

$$V_o/V_i = A(\cos \theta + j \sin \theta) = Y_s/Y_f \quad (1)$$

Defining Y_s and Y_f as a parallel combination of capacitance C_s and conductance G_s , i.e., $Y_s = G_s + j\omega C_s$ and using Eq. (1), we obtain

$$C_s = A\{C_f \cos \theta + (G_f/\omega) \sin \theta\} \quad (2)$$

$$G_s = A(G_f \cos \theta - C_f \omega \sin \theta) \quad (3)$$

The results of preliminary test measurements with this system using cell equivalent circuits with known component values were satisfactory [14].

3. Results

3.1. Myoblast cells

Mononucleated myoblast cells do not have a complex cellular architecture, therefore, the analysis of experimental results is straightforward compared to myotubes. Prior to the measurement, myoblast cells were treated with a dilute trypsin solution in order to alter their shape to well defined spherical geometry. This process was necessary in order to facilitate the determination of the cell surface area. Fig. 2 illustrates the frequency profile of capacitance and conductance of a myoblast cell measured with the micropipet method. The pronounced decrease of capacitance and the increase in conductance at high frequencies are

either partially or entirely due to the series resistance (R_s) as shown by the equivalent circuit in the same figure. The large tip impedance of micropipets is the major source of the series resistance. The membrane capacitance C_m and conductance G_m can be calculated using the following equations [21,22].

$$C_m = \frac{C_m R_m^2 / (R_s + R_m)^2}{1 + (\omega T)^2} \quad (4)$$

$$G_m = \frac{1/(R_s + R_m) + \omega^2 T^2 / R_s}{1 + (\omega T)^2} \quad (5)$$

where T is time constant for the circuit shown in the figure and is given by

$$T = C_m R_s R_m / (R_s + R_m) \quad (6)$$

Using these equations, the systematic error due to a series resistance R_s can be readily corrected. So far, passive cell membranes such as human erythrocytes [23], mouse myeloma and human HeLa cells were found to have a frequency independent capacitance and conductance [14]. In order to determine the value of series resistance R_s , we transform measured admittances into impedance parameters, i.e., resistance R and reactance X . The plot of reactance $-X$ against resistance R is usually circular. The intercept of the impedance arc with the abscissa at high frequency end yields the value of series resistance as shown in Fig. 3. Starting with the value obtained from this plot, the value of R_s is either incremented or decremented with small steps until we reach a satisfactory result.

Fig. 4 shows the corrected capacitance and conductance of myoblast cells using the best R_s value. First of all, the specific capacitance of myoblast membrane is found to be about 2.2–2.5 $\mu\text{F}/\text{cm}^2$ which is larger than the normal value, i.e., 1 $\mu\text{F}/\text{cm}^2$. Also this value is considerably larger than the one reported by Kidokoro, i.e., 1 $\mu\text{F}/\text{cm}^2$ [16]. The source of this dis-

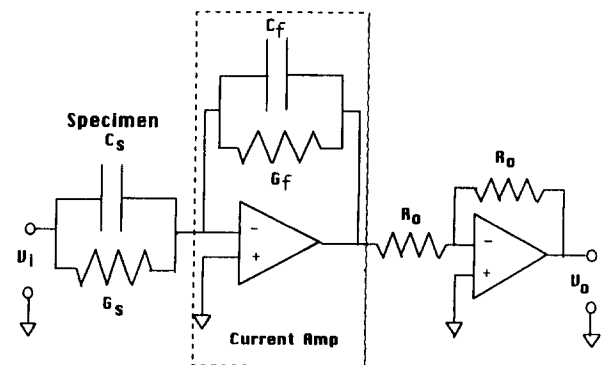


Fig. 1. A schematic diagram of the measuring system. V_i and V_o are input and output voltages, $R_f (= 1/G_f)$ is a feedback resistor and C_f is the parasitic capacitance of the resistor. C_s and G_s are the capacitance and conductance of the sample. The second amplifier represents an inverter circuit.

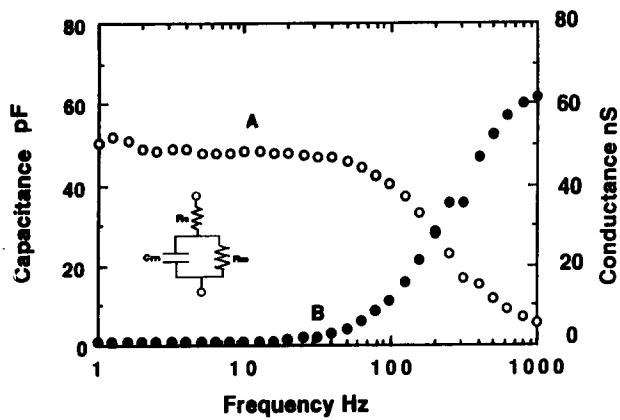


Fig. 2. Frequency profile of the measured capacitance (A) and conductance (B) of a mononucleated myoblast cell. The inset represents an equivalent circuit of a leaky membrane with a capacitance C_m and resistance R_m . R_s is a series resistance which arises mainly from the tip impedance of micropipets.

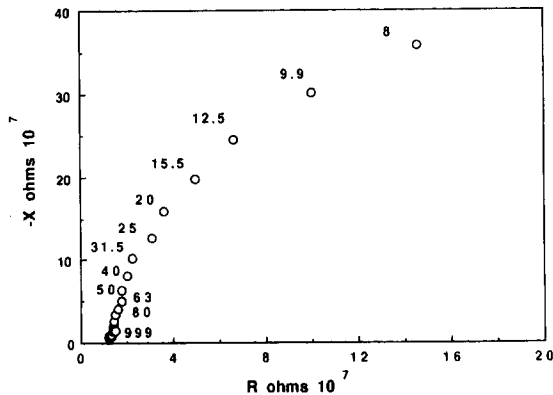


Fig. 3. Complex impedance plot of a myoblast cell. R is resistance and X is reactance in ohms. The intercept of the impedance arc with the abscissa gives the value of series resistance. Starting with this value, fine adjustments were made to find the best value of R_s . Only the high frequency end of the plot is shown. The numbers are frequencies in Hz.

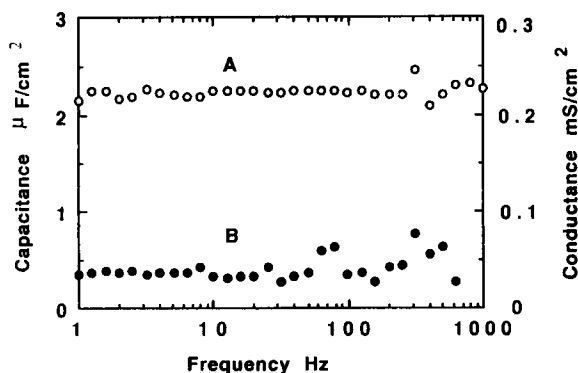


Fig. 4. Frequency profile of the capacitance (A) and conductance (B) of myoblast cells after R_s correction. Note that both capacitance and conductance are independent of frequency.

agreement is still unknown. Eisenberg et al. [9] and Vaughan et al. [7] found the specific capacitance of the surface membrane of frog sartorius muscle, with disruption of the transverse tubular membranes by glycerol or by low ionic strength, to be $2.25 \mu\text{F}/\text{cm}^2$ rather than the usual $1 \mu\text{F}/\text{cm}^2$. Thus the specific membrane capacitance of myoblasts is similar to that of muscle surface membrane.

However, there is a possible explanation for the large apparent membrane capacity of myoblasts. The myoblast cell used for our measurements was treated with trypsin in order to cleave them from the wall of culture dish. Cleaved cells change shape from a flat disc to a sphere without changing their volume. Since the area of membrane is always constant, the only way to achieve this is invagination of the surface of the cells, which is not detected by the low power microscopic determination of the cell size. Consequently the estimate of the cell surface area, because of the neglect of invagination, tends to be smaller than the real surface area. This entails a larger membrane capacitance per unit area. The following simple numerical analysis shows that the correction for the invagination results in a value of about $1 \mu\text{F}/\text{cm}^2$.

If the radius and thickness of disc shaped myoblasts are assumed to be r and h and the radius of spherical cell after the trypsin treatment is R , we readily obtain the following equation by equating the volumes of the cell before and after the trypsin treatment, $R^3 = 3r^2h/4$. The ratio of surface areas of spherical and disc shaped cells is therefore $S'/S = 2R^2/r(r+h)$ (where S and S' are the areas of disc and spherical cells) and the specific capacitance of the spherical cell is $C' = CS/S'$. We assume $r = 30 \mu\text{m}$ and $h = 5 \mu\text{m}$, then $S'/S = 2.33$ and we obtain a value of about $1 \mu\text{F}/\text{cm}^2$ for the true membrane capacity of myoblast cells.

The conductance of $50\text{--}60 \mu\text{S}/\text{cm}^2$, on the other hand, is similar to the one observed by Kidokoro (about $100 \mu\text{S}/\text{cm}^2$).

Secondly, the capacitance and conductance of myoblast membrane, after the correction for the series resistance, were found independent of frequency between 1 Hz and 1 KHz. This behavior is similar to those of passive cells which we studied previously.

3.2. Myotubes

The capacitance and conductance of myotubes without trypsin treatment are illustrated in Fig. 5. These data are corrected for the series resistance R_s . The complex geometries of myotubes often prevented the accurate determination of their size or surface area. Because of this difficulty, the total capacitance instead of specific capacitance is plotted in this figure. The formation of a polynucleated myotube resulted in a

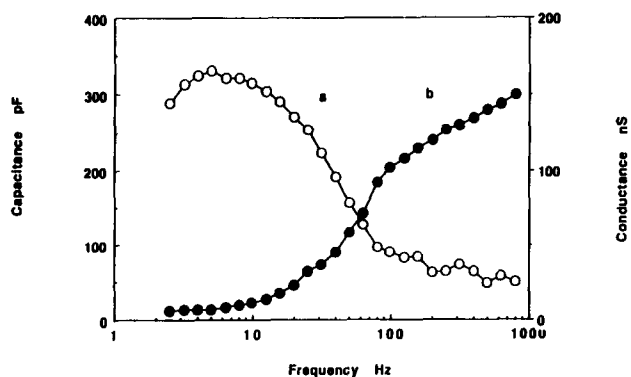


Fig. 5. Frequency profile of the capacitance (a) and conductance (b) of polynucleated myotubes without trypsin treatment. Note the large total capacitance and its marked frequency dependence. Measured capacitance and conductance were corrected for R_s using the circuit shown in Fig. 2 and Eqs. (4) and (5).

marked increase in the total capacitance (about 300–600 pF) and a pronounced frequency dependence. The magnitude of capacitance and the characteristic frequency of the dispersion are remarkably similar to those observed with frog skeletal muscles. The large and frequency dependent capacitance of skeletal muscle cells is attributed to transverse tubules and a number of detailed analyses have been presented by many investigators [3,5,6,8]. Because of this reason, we are able to postulate that the frequency dependent capacitance of myotubes is, similar to muscle cells, due to the presence of a tubule-like structure. A more detailed analysis will follow in a later section.

Fig. 6 illustrates the capacitance of a trypsin treated myotube. Similar to the result shown in Fig. 5, the measured capacitance exhibits a marked frequency dependence. The trypsin treatment changes the cell geometry to a simple disc with a circular or elliptic cross sections thus renders the determination of cell surface area somewhat easier. In spite of this, accurate deter-

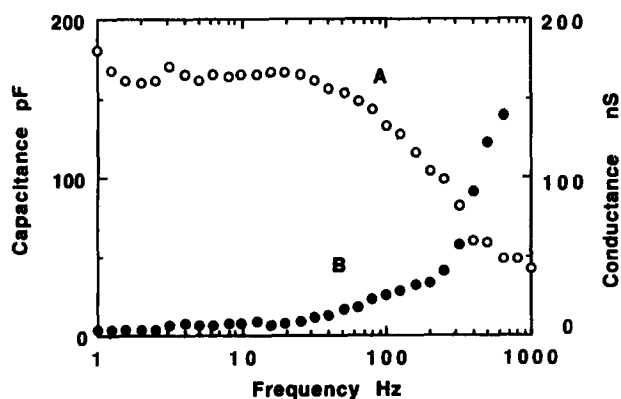


Fig. 6. Frequency profile of the capacitance of polynucleated myotube membrane with trypsin treatment after the correction for R_s . Note the shift of dispersion curve to a higher frequency region. The specific membrane capacitance and conductance are about $5.8 \mu\text{F}/\text{cm}^2$ and $0.43 \text{ mS}/\text{cm}^2$, respectively.

mination of the area of large myotube cells is still difficult because of the uncertainty of cell thickness. The area of this particular cell is roughly estimated to be about $3.45 \cdot 10^{-5} \text{ cm}^2$ assuming that myotube cells are thin flat discs. Using this value, the specific membrane capacitance and conductance of this cell are found to be about $5.8 \mu\text{F}/\text{cm}^2$ and $0.43 \text{ mS}/\text{cm}^2$. These values are similar to those of the transverse tubules in muscle cells and is also in agreement with those reported by Kidokoro [16].

4. Discussion

There are several origins for the frequency dependence of the admittance parameters, i.e., capacitance and conductance of cell membranes. In the following, a brief discussion will be presented in order to facilitate the understanding of this problem.

4.1. Frequency dependence due to series resistance

The membrane admittances which are measured using a pair of electrodes always include a series resistance as shown by the inset of Fig. 2. The series resistance arises from the imperfect contact between metal electrode and membrane surface. In the case of the micropipet technique, the tip impedance of micropipets which is large and in series with the admittance of the membrane causes a marked decrease in measured capacitance and an increase in conductance at high frequencies. Therefore, the correction for R_s is crucial to find the true frequency dependence of admittance components. In case of the mononucleated myoblast cells which have a simple structure, surface membrane is the major component of the total admittance. Because of this, the correction for R_s is relatively easy and its capacitance and conductance are found to be independent of frequency.

Polynucleated myotubes are formed by the fusion of myoblast cells. If fused myotubes have no substructure (such as tubules), then the admittance is represented by the surface membrane alone. In this case, the specific capacitance and conductance of myotubes should be similar to those of myoblast cells. However, the specific capacitance of myotubes is much larger than that of myoblast and markedly frequency dependent in spite of the correction for the series resistance R_s . This clearly indicates that the estimation of the area of cell surface must include some additional areas due to a yet unknown substructure. In other words, the admittances of myotubes must be represented by an equivalent circuit shown in Fig. 7 instead of a simple circuit shown in Fig. 2. The distributed resistors in the lumen of tubules constitute the series resistance to the admittances of tubular membrane. Many lumped circuit

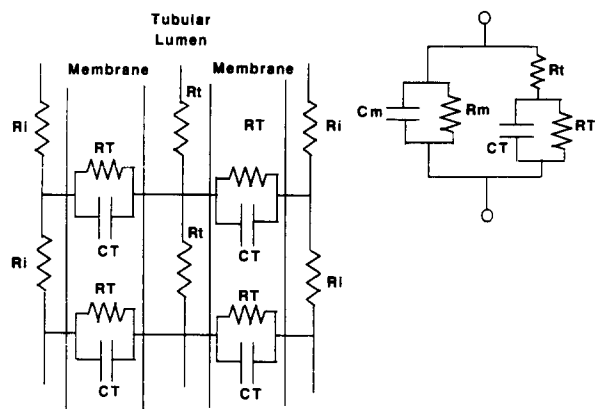


Fig. 7. Distributed capacitance (C_T) and resistance (R_T) elements in the membrane of a tubule-like structure. R_i is the series resistances distributed in the lumen of tubules. The inset shows the equivalent circuit. C_m and R_m are the capacitance and resistance of the surface membrane. Note that this is an admittance circuit which generates Eqs. (7) and (8).

models have been proposed hitherto by various authors to interpret impedance data [24]. We used in a previous paper a lumped circuit in order to explain the admittance data of frog skeletal muscle measured by a vaseline gap technique [25]. This diagram is reproduced by the inset of Fig. 7. C_m and R_m are the capacitance and resistance of the surface membrane. R_i is the lumped resistance of the distributed resistors in the lumen. The component values in this circuit are mostly known provided the capacitance and resistance of tubular membrane are assumed to be the same as those of surface membrane. Only unknown quantity is the resistance of the lumen R_i .

The capacitance (C) and conductance (G) of the overall admittance of this circuit, i.e., $Y = G + j\omega C$ is given by Eqs. (7) and (8).

$$C = C_m + \frac{C_T}{1 + (\omega T_i)^2} \left[\frac{R_T}{R_T + R_i} \right]^2 \quad (7)$$

$$G = G_m + \frac{(\omega^2 R_i C_T^2 R_T^2) + (R_i + R_T)}{1 + (\omega T_i)^2} \left[\frac{1}{R_T + R_i} \right]^2 \quad (8)$$

where C_m and G_m are the capacitance and conductance of surface membrane and C_T and R_T are the capacitance and resistance of tubular membrane. R_i is the resistance of the lumen of the tubule and T_i is time constant for the internal network and is defined by

$$T_i = \frac{R_T R_i C_T}{R_T + R_i} \quad (9)$$

The results of the numerical calculation using Eq. (7) assuming R_i to be 495 ohm cm^2 for the myotube without trypsin treatment (curve a) and 100 ohm cm^2 for trypsin treated myotubes (curve b) are shown in

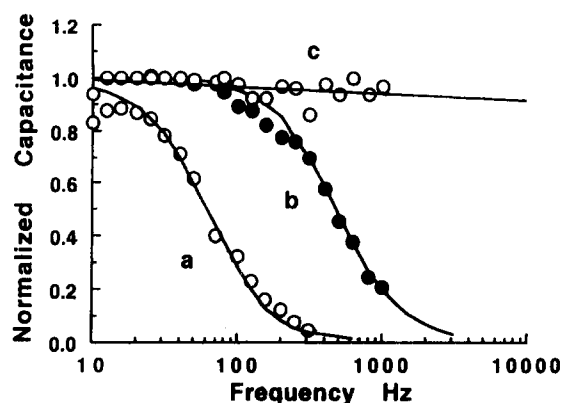


Fig. 8. Normalized capacitances of myotubes calculated using Eqs. (7) and (8). Curve (a) with open circles is for the myotube without trypsin treatment. The solid curve was calculated with $R_i = 495$ ohm cm^2 . Curve (b) with filled circles is for the trypsin treated myotube. The solid line was calculated with $R_i = 100$ ohm cm^2 . Open circles with curve (c) was obtained from curve (b) using a value of R_i of 100 ohm cm^2 in Eq. (7). The straight line is a computer-fitted curve.

Fig. 8 along with measured values. As shown, good agreements are obtained when the value of the resistance of the lumen R_i is carefully chosen. Of particular interest is the observation that the value of R_i of the samples without trypsin treatment tends to be larger than for trypsin treated samples. Curve C with open circles in Fig. 8 are the capacitances after the correction for R_i using Eq. (7). Note that capacitances become frequency independent after this correction. This observation clearly indicates that the apparent frequency dependence of the capacitance of myotubes does not originate from the membrane but is simply due to the series impedance, i.e., the distributed resistors in the lumen as shown in Fig. 7. Table 1 summarizes the mean capacitances and conductances of myoblast and myotube cells.

Although cultured cells do possess, to some extent, physiological properties which resemble those of non-cultured natural muscle cells, nevertheless, the internal structure, even after the formation of multinucleated myotubes, should be much simpler than the full grown natural muscle fibers. Although the present authors as well as Kidokoro suggests the presence of some micro-tubule-like structure in myotubes, we envision that this substructure is rather a primitive one compared to those of natural muscles. Our interest was whether or not the cultured myotubes without an extensive net-

Table 1
Capacitances and conductances of the membranes of myoblasts and myotubes

	Myoblast cells	Myotubes
C_m	1–2 $\mu\text{F}/\text{cm}^2$	5–6 $\mu\text{F}/\text{cm}^2$
G_m	50–60 $\mu\text{S}/\text{cm}^2$	0.4 mS/ cm^2

work of microtubules can simulate the complex admittance and/or impedance behavior of natural muscle cells. As discussed above, the magnitude of membrane capacitance and its frequency characteristics of myotubes are remarkably similar to those observed with skeletal muscles.

4.2. Frequency dependence due to cable attenuation

Although the analysis based on the equivalent circuit shown in Fig. 7 explains the admittance characteristics of myotubes satisfactorily, there is a possible alternate interpretation, based on the cable theory used by Falk et al. [3], for the frequency dependent capacitance and conductance of myotube membranes.

Muscle fibers, natural and/or cultured, with distributed capacitive and conductive elements, can be approximated by transmission lines with either infinite or finite lengths. In general, the propagation of voltage waves along a transmission line can be expressed, using the transmission line theory, by the following equation [26].

$$V = V_1 \exp(-x/\lambda) + V_2 \exp(+x/\lambda) \quad (10)$$

Likewise the current I flowing along the fiber is defined by

$$I = (1/Z_o)V_1 \exp(-x/\lambda) - (1/Z_o)V_2 \exp(+x/\lambda) \quad (11)$$

where λ , propagation constant or length constant, is given by

$$\lambda^2 = 1/(R + j\omega L)(G + j\omega C) \approx 1/R(G + j\omega C) \quad (12)$$

where R and L are series resistance and inductance per unit length of transmission line and G and C are trans-conductance and capacitance. For biological materials, we can assume that the series inductance is negligibly small, hence, the simplification shown in Eq. (12). Z_o is characteristic impedance of the transmission line and is defined by:

$$Z_o^2 \approx \frac{R}{G + j\omega C} \quad (13)$$

For a transmission line of finite length, the reflection coefficient p is given by the following equation if terminal impedance is assumed to be Z_e .

$$p = \frac{Z_e - Z_o}{Z_e + Z_o} \quad (14)$$

Obviously, reflection coefficient reduces to 0 when Z_e is equal to Z_o . For excised muscle preparations with cut ends or those terminated with tendons, Z_e is not the same as Z_o and we will have to consider reflections at the terminal. However, no such heterogeneity exists

for cultured myotubes which are formed by the fusion of myoblasts. Under these circumstances, we can safely assume that $Z_o = Z_e$ and consequently the reflection coefficient p negligibly small or even equals 0. Thus the characteristic impedance or admittance of myotubes can be readily calculated using Eq. (13) by identifying R , G and C as series resistance r_i , trans-membrane conductance G_m and capacitance C_m . Separating real and imaginary parts, we obtain Eqs. (15) and (16).

$$g = \sqrt{1/r_i} \left\{ \sqrt{G_m/2} \left(1 + \sqrt{1 + (C_m \omega / G_m)^2} \right)^{1/2} \right\} \quad (15)$$

$$c = (C_m/2) \sqrt{1/r_i} \times \left\{ \sqrt{2/G_m} \left(1 + \sqrt{1 + (C_m \omega / G_m)^2} \right)^{-1/2} \right\} \quad (16)$$

Eqs. (15) and (16) indicate that measured capacitance and conductance c and g are always frequency dependent even when the distance between two electrodes reduces to zero as long as the size of cells is larger than or comparable to propagation constant. The capacitances at $\omega = 0$ and ∞ are

$$c = (C_m/2) / \sqrt{r_i G_m} \quad \omega \rightarrow 0 \quad (17)$$

$$c = \sqrt{C_m/2r_i} \omega \rightarrow 0 \quad \omega \rightarrow \infty \quad (18)$$

Eqs. (15) and (16) indicate that measured capacitance decreases as the frequency increases between 0 and ∞ regardless of the nature of C_m and G_m and eventually approaches zero.

In conclusion, the frequency dependence of the capacitance of myotube membrane can be explained either by the assumption of a tubular-like substructure or by the use of cable equation. The presence of a substructure in myotubes, however, has not been proven by independent means such as electron microscopy. It is, therefore, important to undertake this endeavor before we accept this hypothesis. On the other hand, the length constants in excitable cells are of the order of 4–6 mm and is much larger than the dimension of myotubes. Thus the voltage attenuation which is dictated by Eq. (10) may not be substantial. Therefore, the applicability of the cable theory to myotubes is only marginal.

5. Acknowledgement

K.A. is a recipient of the Yamada Foundation Fellowship.

6. References

- [1] Guttman, R. (1939) J. Gen. Physiol. 50, 2437–58.
- [2] Schwan, H.P. (1954) Z. Naturforsch. 9, 245–251.

- [3] Falk, G. and Fatt, P. (1964) *Proc. R. Soc. Lond. B*, 160, 69–130.
- [4] Freygang, W.H., Rappoport, S.I. and Peachey, L.D. (1967) *J. Gen. Physiol.* 50, 2437–2458.
- [5] Eisenberg, R.S., Vaughan, P.C. and Howell, J.N. (1972) *J. Gen. Physiol.* 59, 360–373.
- [6] Validiosa, R., Clausen, C. and Eisenberg, R.S. (1974) *J. Gen. Physiol.* 63, 432–457.
- [7] Vaughan, P.C., Howell, J.N. and Eisenberg, R.S. (1972) *J. Gen. Physiol.* 59, 347–359.
- [8] Gage, P.W. and Eisenberg, R.S. (1969) *J. Gen. Physiol.* 59, 347–359.
- [9] Eisenberg, R.S. and Gage, P.W. (1967) *Science* 158, 1700–1701.
- [10] Eisenberg, B. and Eisenberg, R.S. (1968) *J. Cell Biol.* 39, 451–467.
- [11] Gage, P.W. and Eisenberg, R.S. (1969) *J. Gen. Physiol.* 53, 298–310.
- [12] Hille, B. and Cambell, D.T. (1976) *J. Gen. Physiol.* 67, 265–293.
- [13] Nelson, G.P. and Lieberman, M. (1981) *Excitable Cells in Tissue Culture*, Plenum Press, New York.
- [14] Asami, K., Takahashi, Y. and Takashima, S. (1990) *Biophys. J.* 58, 143–148.
- [15] Kidokoro, Y. (1981) in *Excitable Cells in Tissue Culture* (Nelson, G.P. and Lieberman, M., eds.), Plenum Press, New York.
- [16] Kidokoro, Y. (1981) in *Excitable Cells in Tissue Culture* (Nelson, G.P. and Lieberman, M., eds.), Plenum Press, New York.
- [17] Kidokoro, Y. (1973) *Nature (New Biology)* 241, 158.
- [18] Kidokoro, Y. (1975a) *J. Physiol.* 244, 129.
- [19] Milton, R.L., Mathias, R.T. and Eisenberg, R.S. (1985) *Biophys. J.* 48, 253–267.
- [20] Sakmann, B. and Neher, E. (1983) *Single Channel Recording*, Plenum Press, New York.
- [21] Takashima, S. and Schwan, H.P. (1974) *J. Membr. Biol.* 17, 51–68, 1974.
- [22] Takashima, S. (1989) *Electrical Properties of Biopolymers and Membranes*, Ch. 8, pp. 242, Adam Hilger, Bristol.
- [23] Takashima, S., Asami, K. and Takahashi, Y. (1988) *Biophys. J.* 54, 995–1000.
- [24] Schanne, O.F. (1978) *Impedance Measurements in Biological Cells*, Ch. 3, pp. 136–201, John Wiley, New York.
- [25] Takashima, S. (1985) *Pflügers Arch.* 403, 197–204.
- [26] Schwan, H.P. (1963) in *Physical Techniques in Biological Research*, Vol. 6, Ch. 6, (Nastuk, W.L., ed.), Academic Press, New York.